Predictive Torque Control Strategy of an Open-End Winding Induction Motor Drive with Less Common-Mode Voltage

Kunisetti V Praveen Kumar
Electrical Engineering
NIT Warangal
Warangal, India
kvpraveenkumar15@gmail.com

Thippiripati Vinay Kumar
Electrical Engineering
NIT Warangal
Warangal, India
tvinay.nitw@gmail.com

***Abstract*— Direct Torque Control (DTC) and Predictive Torque Control (PTC) Strategies emerged as popular techniques for speed control of Induction Motor Drives. In this article, an effective PTC strategy is introduced to an Open-End Winding Induction Motor Drive (OEWIMD) to control torque and flux directly. PTC offers all the features of classical DTC and it provides lesser ripple in torque and flux. The limitations of classical PTC are: (i) higher common-mode voltage (ii) variable switching frequency (iii) high computational burden and (iii) selection of weighting factors. To trounce some of these problems PTC of OEWIMD is developed. OEWIMD is operated with dual inverter configuration. In dual inverter configuration, if the inverters are operated with equal DC bus voltages (1:1 ratio), it can deliver '18' space vector locations, out of these space vector locations only six active space vectors and a null vector has been considered. The voltage vectors used to implement the proposed algorithm can maintain less common-mode voltage. The proposed algorithm is verified by comparing the obtained experimental results with simulation results.**

Keywords—Direct Torque Control, Predictive Torque Control, Open-End Winding Induction Motor Drive, Torque Control, Flux Control and Common-mode Voltage

I. Introduction

Most of the industrial applications rely on variable speed drives (VSD). The VSD should provide high dynamic performance and ease of control. VSD are generally employed with field oriented control (FOC) or direct torque control. The DTC strategy is initiated by Takahashi and Nogouchi, to overcome the limitations of FOC [1]. FOC involves complex co-ordinate transformation, rotor flux observer and the control algorithm has to be developed in synchronous reference frame. These limitations can be easily replaced by DTC, since it involves the implementation of control algorithm in stationary reference frames [2]. The classical DTC has several limitations: (i) the use of hysteresis controllers causes variable switching frequency, (ii) Higher ripples in torque and flux and (iii) possible problems during starting and low speeds. To address these problems and also to obtain all the features of classical DTC, predictive torque control has been developed. PTC combines the features of DTC and model predictive control (MPC) [3]. The working principle of PTC is same as DTC whereas it offers lesser ripples in torque and flux, by using discrete models of inverter and AC motor [4]. In recent days, PTC became an interesting area for researchers due to its wide advantages. The advantages of PTC are decoupled control of torque and flux, easy inclusion of constraints in cost function, ease of control and simplicity. Many of the research articles have been proposed in the PTC of induction motor drives to reduce torque and flux ripples, some of the researchers addressed reduction of common-mode voltage. In [5], dead-beat controlled PTC of induction motor drive has been introduced to reduce torque and flux ripple. It needs a special PI controller and a modulator. Immediate flux control based PTC of induction motor is developed to reduce switching frequency [6]. It requires complex equations and does not account torque and flux ripples.

The concept of Model predictive torque control of induction motor drives by using extrapolation method was introduced to a three-level neutral point clamped (NPC) inverter [7]. The torque and flux ripple in PTC is due to the application of voltage space vector for one complete control cycle. In [8], variable switching time point based PTC strategy has been introduced to reduce torque and flux ripples. An improvised PTC of induction motor by using duty-ratio control technique is developed [9]. It involves computation of the time required for the application of active voltage space vector and null vector. In [10], a novel angle controlled PTC scheme has been introduced. It uses the angle between stator current and rotor flux to predict the torque. The torque and current equations of the induction motor drive are independent of stator voltage space vector.

From the literature, it has been found that torque and flux ripples of induction motor drive can be reduced by using multi-level inversion or duty cycle control or addition of constraints into the cost function. In this article, PTC of an OEWIMD is introduced to reduce common-mode voltage by applying selective voltage space vectors. OEWIMD has several features over conventional induction motor drives. OEWIMD itself can provide mutli-level output voltage by using only two two-level inverters. OEWIMD can provide multi-level inversion by using less number of switches. When compared with other multi-level inversion (MLI) topologies, In NPC inverters, there exist voltage fluctuations at neutral point and also requires clamping diodes [11]. OEWIM can be operated even in fault conditions [12]. OEWIMD is better alternative and it provides all the features offered by other MLI topologies. Dual inverter fed OEWIMDs has several applications: (i) Hydrid electric vehicle [13] (ii) ship propulsion [14] and (iii) Renewable energy integration [15]. In [16], DTC of OEWIMD has been implemented by a novel switching state algorithm. In [17], PTC of OEWIMD was introduced with MLI output voltage. This article uses a modified cost function to reduce common-mode voltage.

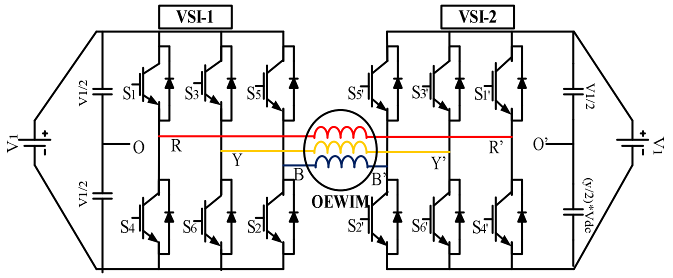

Fig. 1. Power Circuit of dual inverter fed OEWIMD.

In this article, PTC strategy of an OEWIMD introduced to reduce common-mode voltage, torque and flux ripple. The proposed algorithm utilises only 7 switching states out of 18 space vector locations to reduce computational burden and switching frequency. The intents of the proposed PTC algorithm are: (i) Discrete implementation of Open end winding induction motor (ii) Discrete model of dual inverter configuration (iii) formulation of voltage space vectors to deliver less common-mode voltage and (iv) optimisation of cost function.

The organisation of this article is as follows. This article contains five parts. Introduction part describes the advantages of proposed PTC strategy in contrast to other PTC algorithms. Part II briefly explains the implementation OEWIMD. Part III is to discuss the implementation of proposed PTC algorithm and its implementation. To show the effectiveness of proposed PTC strategy experimental studies has been carried. Part IV describes comparative analysis of simulation and experimental results. Finally part V describes the objectives of the proposed PTC strategy in terms of conclusions.

II. Dynamic Model of OEWIMD and Inverter

A. Dynamic model of Dual inverter configuration

The configuration of dual inverter fed OEWIMD is as shown in Fig.1. Dual inverter is operated with equal DC-link voltage (1:1 ratio). By operating the dual inverter configuration with equal DC link voltage, it delivers two-level and three-level output voltage with 18 active voltage space vector locations. The proposed algorithm utilizes only 7 space vector locations, out of these 6 space vector locations are active voltage vector and one zero vector. The dynamic model of dual inverter configuration is given by (1) to (5).

The pole voltages of dual inverter configuration shown in Fig. 1 can be written as (1) and (2).

$$\begin{pmatrix} V_{ro} \\ V_{yo} \\ V_{bo} \end{pmatrix} = (V_1) \begin{pmatrix} S_r \\ S_y \\ S_b \end{pmatrix} \tag{1}$$

$$\begin{pmatrix} V_{r'o'} \\ V_{y'o'} \\ V_{b'o'} \end{pmatrix} = (V_1) \begin{pmatrix} S_{r'} \\ S_{y'} \\ S_{b'} \end{pmatrix} \tag{2}$$

$$\begin{pmatrix} dV_{rr'} \\ dV_{yy'} \\ dV_{bb'} \end{pmatrix} = \begin{pmatrix} V_{ro} - V_{r'o'} \\ V_{yo} - V_{y'o'} \\ V_{bo} - V_{b'o'} \end{pmatrix} \tag{3}$$

The pole voltages of inverter-1 are given by (1), whereas (2) describes the pole voltages of inverter-2. The difference of pole voltages is given by (3). To obtain common-mode voltage of dual inverter configuration it is necessary to use difference of pole voltages (3). From (3), the common-mode voltage (CMV) can be written as (4)

$$V_c = \left(\frac{1}{3}\right)\left(dV_{rr'} + dV_{yy'} + dV_{bb'}\right) \tag{4}$$

The phase voltages of dual inverter configuration can be written by using (3) and (4). The phase voltages of dual inverter configuration are given by (5) and it can also be written as (6).

$$\begin{pmatrix} V_{rr'} \\ V_{yy'} \\ V_{bb'} \end{pmatrix} = \begin{pmatrix} dV_{rr'} - V_c \\ dV_{yy'} - V_c \\ dV_{bb'} - V_c \end{pmatrix} \tag{5}$$

$$\begin{pmatrix} V_{rr'} \\ V_{yy'} \\ V_{bb'} \end{pmatrix} = \frac{1}{3} \begin{pmatrix} 2 & -1 & -1 \\ -1 & 2 & -1 \\ -1 & -1 & 2 \end{pmatrix} \begin{pmatrix} dV_{rr'} \\ dV_{yy'} \\ dV_{bb'} \end{pmatrix} \tag{6}$$

B. Discrete Model of OEWIMD

Discrete model of OEWIMD is implemented in stationary reference frames. The proposed PTC strategy implements the control algorithm in stationary reference frames, whereas FOC requires control algorithm in synchronous reference frame. The discrete model of OEWIMD is shown in Fig. 2. The discrete model of OEWIMD is given by (7)-(12).

The stator and rotor voltages of OEWIMD in stationary reference frame are given by (7) and (8), whereas (9) and (10) gives stator and rotor flux.

$$\begin{pmatrix} V_{s\alpha}(k) \\ V_{s\beta}(k) \end{pmatrix}_m = R_s \begin{pmatrix} i_{s\alpha}(k) \\ i_{s\beta}(k) \end{pmatrix}_m + p \begin{pmatrix} \psi_{s\alpha}(k) \\ \psi_{s\beta}(k) \end{pmatrix}_m \tag{7}$$

$$\begin{pmatrix} 0 \\ 0 \end{pmatrix}_m = R_r \begin{pmatrix} i_{r\alpha}(k) \\ i_{r\beta}(k) \end{pmatrix}_m + p \begin{pmatrix} \psi_{r\alpha}(k) \\ \psi_{r\beta}(k) \end{pmatrix}_m + \omega_r \begin{pmatrix} \psi_{r\beta}(k) \\ -\psi_{r\alpha}(k) \end{pmatrix}_m \tag{8}$$

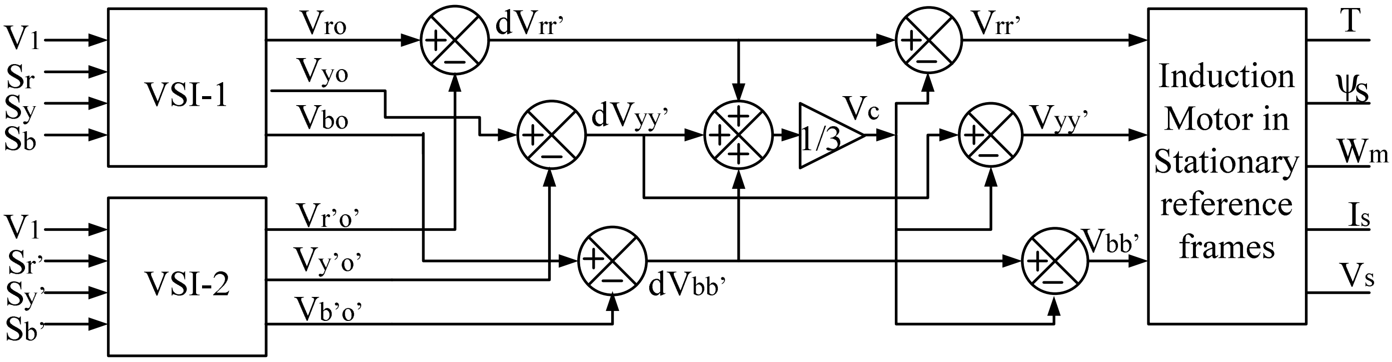

Fig. 2. Discrete Model of OEWIMD.

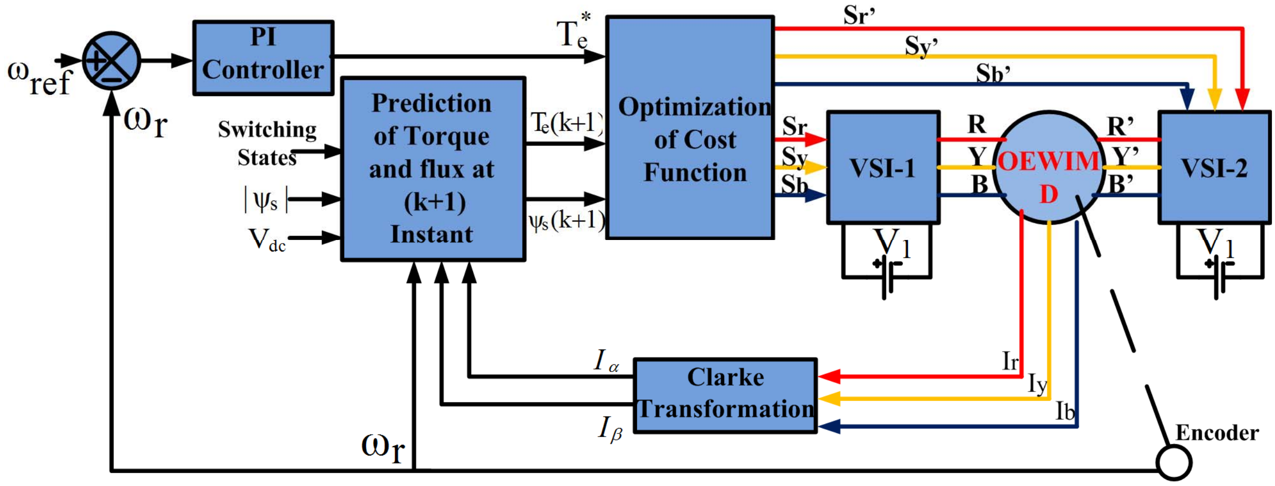

Fig.3. Proposed PTC strategy of OEWIMD with dual inverter configuration.

$$\begin{pmatrix}\psi_{s\alpha}(k)\\ \psi_{s\beta}(k)\end{pmatrix}_m = L_s\begin{pmatrix}i_{s\alpha}(k)\\ i_{s\beta}(k)\end{pmatrix}_m + L_m\begin{pmatrix}i_{r\alpha}(k)\\ i_{r\beta}(k)\end{pmatrix}_m \quad (9)$$

$$\begin{pmatrix}\psi_{r\alpha}(k)\\ \psi_{r\beta}(k)\end{pmatrix}_m = L_r\begin{pmatrix}i_{r\alpha}(k)\\ i_{r\beta}(k)\end{pmatrix}_m + L_m\begin{pmatrix}i_{s\alpha}(k)\\ i_{s\beta}(k)\end{pmatrix}_m \quad 10)$$

From (7)-(10), the electromagnetic torque of OEWIMD can be written as (11), the speed of OEWIMD is given by (12) and it is obtained by using mechanical model of OEWIMD.

$$T(k)_m = \left(\frac{3}{2}\right)\left(\frac{P}{2}\right)\left(\psi_{s\alpha}(k)_m i_{s\beta}(k)_m - \psi_{s\beta}(k)_m i_{s\alpha}(k)_m\right) \quad (11)$$

$$J\frac{d\omega_m}{dt} = T(k)_m - T_l \quad (12)$$

In (7)-(12) 'p' indicates d/dt, ω_m indicates mechanical speed.

III. Proposed Predictive Torque Control Strategy

The block diagram used to implement proposed PTC strategy is shown in Fig. 3. In this article, proposed PTC strategy is developed with '6' active voltage vector and one zero voltage vector. The voltage space vector of inverter-1 is given by (13), whereas (14) gives voltage space vector of inverter-2.

$$V_{o1} = \left(\frac{2}{3}\right)(V_1)\left(S_r + S_y e^{j2\pi/3} + S_b e^{j4\pi/3}\right) \quad (13)$$

$$V_{o2} = \left(\frac{2}{3}\right)(V_1)\left(S_{r'} + S_{y'} e^{j2\pi/3} + S_{b'} e^{j4\pi/3}\right) \quad (14)$$

The resultant voltage space vector of dual inverter fed OEWIMD can be written as (15)

$$V_o = V_{o1} - V_{o2} \quad (15)$$

The resultant voltage space vector diagram of dual inverter fed OEWIMD is shown in Fig. 4.

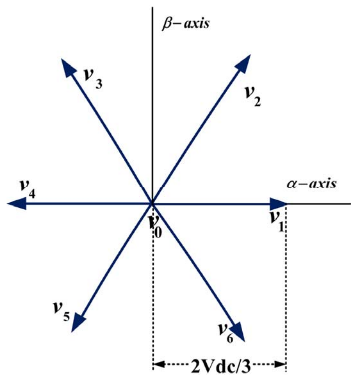

Fig. 4. Location of active voltage space vectors of OEWIMD.

Table I depicts, realization of active voltage space vectors and the CMV associated with respective voltage vectors of OEWIMD.

TABLE I. Realization of active voltage vectors and their CMV

Inverter-1 (S_r, S_y, S_b)	Inverter-2 ($S_{r'}$, $S_{y'}$, $S_{b'}$)	CMV	Voltage Vector	Realization of voltage Space Vector
		V_c	Vo	V_o
0 0 0	0 0 0	0	V_0	0
1 0 0	0 1 1	$-V_{dc}/6$	V_1	$0.667*V_{dc}$
1 1 0	0 0 1	$V_{dc}/6$	V_2	$V_{dc}*(0.333+0.577j)$
0 1 0	1 0 1	$-V_{dc}/6$	V_3	$V_{dc}*(-0.333+0.577j)$
0 1 1	1 0 0	$V_{dc}/6$	V_4	$-0.667*V_{dc}$
0 0 1	1 1 0	$-V_{dc}/6$	V_5	$V_{dc}*(-0.333-0.577j)$
1 0 1	0 1 0	$V_{dc}/6$	V_6	$V_{dc}*(0.333-0.577j)$

In Table I, '1' indicates top switch of respective leg is ON, whereas '0' indicates bottom switch of respective leg is ON. With the help of switching states shown in Table I, the location of active voltage space vectors is shown in Fig. 4. From Table I it is evident that the proposed PTC strategy develops less CMV, when compared with classical PTC strategy of induction motor drive [3]. In classical PTC of induction motor, the CMV is $\pm V_{dc}/3$ and $\pm V_{dc}/2$, whereas the CMV involved in proposed PTC strategy is 0 and $\pm V_{dc}/6$. In classical PTC of induction motor it is very difficult to reduce CMV, whereas by using OEWIMD it is easy to reduce CMV. The feature of OEWIMD with equal DC link voltage is for zero voltage vector it gives '0' CMV, whereas in classical two-level inverter fed induction motor drive the CMV associated with zero voltage space vector is $\pm V_{dc}/2$. By using the voltage space vectors shown in Table I, the proposed PTC strategy has been developed.

A. Prediction of control variables

Once the realization of active voltage space vectors is obtained, then it is easy to predict the control variables required for the implementation of proposed PTC strategy. The control variables used to implement proposed PTC strategy are torque and stator flux. To predict the control variables, it is necessary to measure and estimate the variables. Speed, current and voltage are measured by using encoders and sensors. The flux at k^{th} state is estimated by using voltage and current at that instant.

To estimate and predict the control variables forward euler's approach (16) is used.

$$\frac{dX}{dt} = \frac{X(k+1) - X(k)}{T_s} \tag{16}$$

By using (16), the control variables at (k+1) instant can be represented by using (17)

$$X(k+1) = \frac{dF}{dt} T_s + X(k) \tag{17}$$

From (17) and (7), the stator flux at (k+1) instant can be written as

$$\begin{pmatrix} \psi_{s\alpha}(k+1) \\ \psi_{s\beta}(k+1) \end{pmatrix}_m = T_s \begin{pmatrix} \begin{pmatrix} V_{s\alpha}(k) \\ V_{s\beta}(k) \end{pmatrix}_m - \\ R_s \begin{pmatrix} i_{s\alpha}(k) \\ i_{s\beta}(k) \end{pmatrix}_m \end{pmatrix} + \begin{pmatrix} \psi_{s\alpha}(k) \\ \psi_{s\beta}(k) \end{pmatrix}_m \tag{18}$$

$$\begin{pmatrix} i_{s\alpha}(k+1) \\ i_{s\beta}(k+1) \end{pmatrix}_m = T_s \begin{pmatrix} E\begin{pmatrix} \psi_{r\alpha}(k) \\ \psi_{r\beta}(k) \end{pmatrix}_m - F\begin{pmatrix} i_{s\alpha}(k) \\ i_{s\beta}(k) \end{pmatrix}_m + \\ G\begin{pmatrix} \psi_{r\beta}(k) \\ -\psi_{r\alpha}(k) \end{pmatrix}_m + \frac{1}{D}\begin{pmatrix} V_{s\alpha}(k) \\ V_{s\beta}(k) \end{pmatrix}_m \end{pmatrix} + \begin{pmatrix} i_{s\alpha}(k) \\ i_{s\beta}(k) \end{pmatrix}_m \tag{19}$$

$$T(k+1) = \left(\frac{3}{2}\right)\left(\frac{P}{2}\right)\begin{pmatrix} \psi_{s\alpha}(k+1) i_{s\beta}(k+1) - \\ \psi_{s\beta}(k+1) i_{s\alpha}(k+1) \end{pmatrix} \tag{20}$$

Where $A = \frac{L_r}{L_m}$, $B = \left(L_m - \frac{L_s L_r}{L_m}\right)$, $C = \left(\frac{L_m R_r}{L_r}\right)$,

$D = \left(\frac{L_s L_r - L_m^2}{L_r}\right)$, $E = \left(\frac{L_m R_r}{L_r^2 D}\right)$,

$F = \frac{L_m}{L_r D}\left(\frac{L_m R_r}{L_r} + \frac{R_s L_r}{L_m}\right)$ and $G = \left(\frac{L_m}{L_r D}\right)$.

B. Cost function formulation and its optimization

The switching states of OEWIMD obtained by optimizing the cost function for every switching state shown in Table I. The cost function (21) is evaluated for all possible switching states (m=1, 2..7) of dual inverter fed OEWIMD.

$$g = \left|T_{ref} - T_{k+1}\right| + \lambda\left|\psi_{sref} - \psi_s(k+1)\right| \tag{21}$$

In (21), λ indicates flux weighting factor. The selection of weighting factor plays a vital role on the performance of OEWIMD. In this article, the value of λ is chosen as '75'. The cost function shown in (21) does not contain CMV term.

The proposed PTC strategy is developed with '7' switching states. The cost function used in the proposed PTC strategy is simple. As the number of switching states is less the switching frequency is also less when compared with classical PTC of induction motor drive.

IV. Simulation and Experimental Results

The effectiveness of the proposed PTC strategy is verified by implementing in MATLAB/SIMULINK and the obtained simulation results are compared with experimental results. An experimental study has been performed by implementing the proposed PTC strategy with dSPACE 1104 controller. The parameters of OEWIMD used for simulation and experimentation are shown in Appendix. Fig. 5-8 describes the simulation and experimental results of proposed PTC strategy.

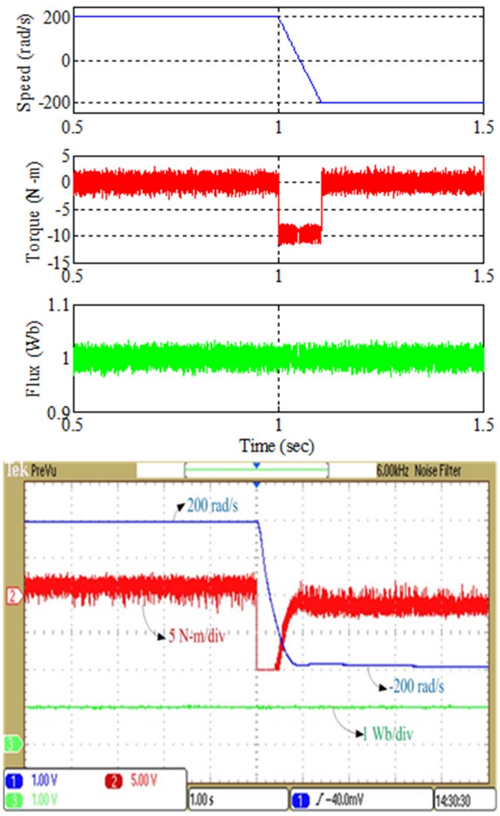

Fig. 5. Simulated (top) and experimental (bottom) results of OEWIMD for speed variations of 200 rad/s to -200 rad/s.

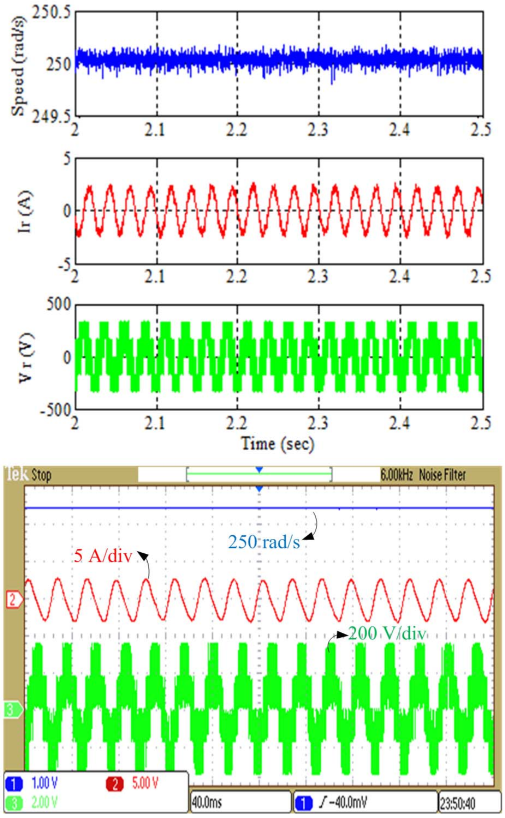

Fig. 6. Simulated (top) and experimental (bottom) results of R-phase current and voltage of OEWIMD at a speed of 250 rad/s.

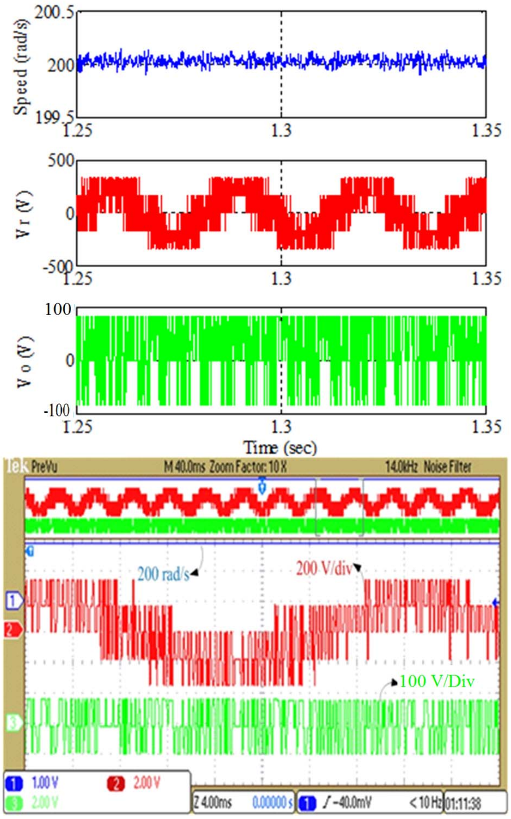

Fig.7. Simulated (top) and experimental (bottom) results of R-phase voltage, CMV at a speed of 200 rad/s.

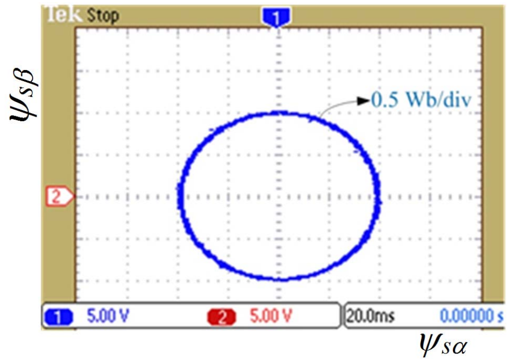

Fig. 8. Experimentally obtained flux locus of OEWIMD.

Fig. 5 demonstrates the dynamic response of torque and flux of OEWIMD with proposed PTC strategy for the speed variation of 250 rad/s (forward motoring) to -250 rad/s (reverse motoring). Fig. 6 demonstrates R-phase current and R-phase voltage of OEWIMD at a steady-speed of 250 rad/s. Fig. 7 demonstrates R-phase voltage and CMV of OEWIMD. From Fig. 7 it is evident that the proposed PTC develops the CMV of 0 V and ±83.33 V (simulation and experimental results), whereas a classical PTC of induction motor delivers CMV of ±250 V and ±177 V. Fig. 8 demonstrates flux locus of OEWIMD at a steady speed of 250 rad/s. From Fig. 5 to Fig. 8, it is evident that the proposed PTC strategy can provide high dynamic performance and gives all the features of classical DTC and PTC with lesser CMV. The proposed PTC strategy can be implementable for more than two-level inversion. In this article, PTC strategy has been shown for two-level inversion.

V. CONCLUSION

In this article, an enhanced PTC strategy of an OEWIMD is developed to reduce common-mode voltage by maintaining all the features of classical PTC. This article suggests an idea to reduce the CMV of induction motor drives by using OEWIMD. The voltage space vectors used to implement the proposed PTC strategy are only '7', hence it involves lower computational burden and the cost function does not require additional terms to reduce CMV. To verify the effectiveness of the proposed PTC strategy, OEWIMD operated in forward and reverse motoring modes. In interest of brevity, the simulation and experimental results are shown for the speeds of 200 rad/s and 250 rad/s. Finally, an effective PTC strategy was developed to reduce the CMV by maintaining the similar characteristics of classical PTC.

APPENDIX

The parameters of OEWIMD used for simulation and experimental verification are: R_s=4.2 Ω, R_r= 2.67 Ω, L_s= 0.54 H, L_r= 0.54 H, L_m= 0.512 H, P=4, J= 0.031 kg/m^2 V_{dc}= 500 V and sample time Ts=65 μs. The test set-up used for experimentation shown in Fig. A.1.

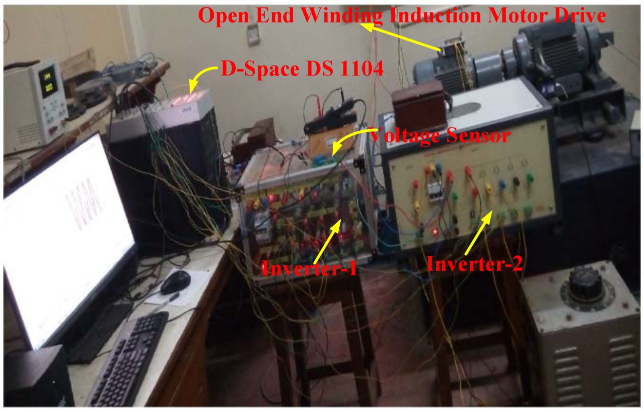

Fig. A.1. Experimental Test Set-up

REFERENCES

[1] Takahashi. I and Noguchi. T., "A new quick-response and high efficiency control strategy of an induction motor," IEEE Trans. Ind. Applicat., vol. 22, no. 5, pp. 820–827, 1986.

[2] D. Casadei, F. Profumo, G. Serra and A. Tani, "FOC and DTC: two viable schemes for induction motors torque control," in *IEEE Transactions on Power Electronics*, vol. 17, no. 5, pp. 779-787, Sep 2002.

[3] H. Miranda, P. Cortés, J. I. Yuz, and José Rodríguez, "Predictive Torque Control of Induction Machines Based on State-Space Models," IEEE Trans. Ind. Elec. vol.56. no.6. June 2009, pp: 1916-1924.

[4] Md. Habibullah, D. Dah-Chuan Lu and Md. Fazlur Rahman "A Simplified Finite-State Predictive Direct Torque Control for Induction Motor Drive," IEEE Trans. Ind. Elec, vol.63, no.6, June 2016, pp: 3964-3975.

[5] Correa. P, M. Pacas and Jose Rodriguez, "Predictive Torque Control for Inverter-Fed Induction Machines," IEEE Trans. Ind. ELEC, vol. 54, no. 2, April 2007, pp: 1073-1079.

[6] M. Nemec, D. Nedeljkovic, and Vanja Ambrozic, "Predictive Torque Control of Induction Machines Using Immediate Flux Control," IEEE Trans. Ind. Elec., vol. 54, no.4, Aug 2007, pp: 2009-2017.

[7] T. Geyer, G. Papafotiou and M. Morrari, "Model Predictive Direct Torque Control—Part I: Concept, algorithm and analysis," IEEE Trans. Ind. Electron., vol. 56, no. 6, June 2009, pp: 1894-1905.

[8] P. Karamanakos, P. Stolze, R. M. Kennel¸ S. Manias and H. D. T. Mouton, "Variable Switching Point Predictive Torque Control of Induction Machines," IEEE Journal of Emerg. And Sele. Topics in Power Electronics, Vol.2, No.2, June 2014, pp: 285-295.

[9] Y. Zhang and H. Yang, "Model Predictive Torque Control of Induction Motor Drives With Optimal Duty Cycle Control," IEEE Trans. Power Electronics, Vol.29, No. 12, Dec-2014, pp: 6593-6603.

[10] S. Alireza Davari, "Predictive Direct Angle Control of Induction Motor," IEEE Trans. Ind. Elect., Vol.63, No.8, Aug-2016, pp: 5276-5284.

[11] Suresh L, Nagarjun S, V. T. Somasekhar, "Improvised SVPWM Strategies for an Enhanced Performance for a Four-Level Open-End Winding Induction Motor Drive," IEEE Trans. Ind. Elect., vol. 64, no.4, pp. 2750-2759, April 2017.

[12] V. T. Somasekhar E. G. Shivakumar K. Gopakumar and A. Pittet, "Multi level voltage space phasor generation for an open-end winding induction motor drive using a dual inverter scheme with asymmetrical DC-link voltages" Eur. Power Electron. Drives, vol. 12 no. 3 pp. 21-29 Jun. 2002.

[13] Abbas Dehghani Kiadehi, Khalil El Khamlichi Drissi, and Christophe Pasquier, "Angular Modulation of Dual-Inverter Fed Open-End Motor for Electrical Vehicle Applications" *IEEE Trans. Power Electron.*, vol. 31, no. 4, pp. 2980 – 2990, Apr. 2016.

[14] Shuai Lu, and Keith Corzine, "Multilevel multi-phase propulsion drives," in Proc. *IEEE Electric Ship Technologies Symposium (ESTS)*, Philadelphia, PA, pp. 363-370, Jul. 2005.

[15] V. Fernao Pires, J. F. Martins, Chen Hao, "Dual-inverter for grid connected photovoltaic system: modeling and sliding mode control" *Solar Energy*, vol.86, Iss. 7, pp. 2106–2115, May 2012.

[16] K. V. Praveen Kumar and T. Vinay Kumar, "Experimental implementation of Direct Torque Control of Open End Winding Induction Motor," In conference Proceedings: TENCON-2016, Singapore, pp. 3318-3323.

[17] Kunisetti V Praveen Kumar and T Vinay Kumar, "Predictive torque control of open-end winding induction motor drive fed with multilevel inversion using two two-level inverters," IET-Electric Power Applications, Vol. 12, No. 1, pp. 54-62, Jan 2018.